Jestr

Journal of Engineering Science and Technology Review 12 (3) (2019) 190 - 200

Research Article

JOURNAL OF
Engineering Science and Technology Review

www.jestr.org

Agricultural Environment Monitoring Combined with Quadrotor Aircraft Control Algorithm

Shen Kefei[1], Li Baoying[1,*], Liu Hanxu[2] and Li Chen[2]

[1]*School of Information Science and Engineering, Dalian Polytechnic University, Dalian 116034, China*
[2]*School of Electrical Engineering and Telecommunications, University of New South Wales, UNSW Sydney, NSW 2052, Australia*

Received 6 January 2019; Accepted 24 June 2019

Abstract

The real-time monitoring of the environment data of crop growth and the status of crop maturity and fruit and vegetable image information is necessary in traditional agricultural production. However, the monitoring methods of crop growth are mostly aimed at individual monitoring rather than overall monitoring. The scope of manual monitoring is often limited because of area, environment, and weather. Moreover, manual monitoring is time-consuming and laborious, and universality is a prominent issue, and they lead to reduced certainties of agricultural environmental monitoring and deviations in data collection. Consequently, the mechanism and control algorithm in large-scale farm environment monitoring based on the quadrotor aircraft was proposed. STM32 was used as the core controller, and the proposed algorithm was combined with the OpenCV pattern recognition module, the 5.8 G wireless image transmission module, and the 2.4 G wireless data transmission module. The control system processed the agricultural image information and analysed the pesticide concentration and environmental temperature and humidity in the growing fruit and vegetable environment to control and monitor the agricultural environment. The accuracy of the selected control algorithm was verified by experimental data. Results demonstrate that the quadrotor aircraft can realize high-precision autonomous flight according to satellite positioning and the image recognition of low-altitude ground signs. The quadrotor aircraft can also independently monitor agricultural environment data by collecting high-definition images of fruits and vegetables and transmit the data and images to the ground station by wireless communication technology. This study provides references in the fields of system modelling, data processing, and control strategy to solve the contradiction between the low efficiency of manual monitoring and the randomness of data acquisition in extensive agricultural areas, subsequently realizing the application of quadrotor aircraft in agricultural monitoring.

Keywords: Agricultural monitoring, Quadrotor aircraft, STM32, PID control algorithm, Pattern recognition

1. Introduction

Fertilization and crop growth monitoring are implemented by experience in most agricultural operations. However, with the passage of time, the experience of planting has become neglected; although the impact is low in small-scale agricultural production, a misjudgment of experience can substantially increase economic loss in large-scale agricultural production [1]. The use of autonomous quadrotor aircraft can change the long-term subjective judgment of agricultural monitoring and management, mainly because such an aircraft can collect data on temperature, humidity, fertility, pests, and pattern information, which then can be analyzed to achieve intelligent perception of agricultural production and provide early warning about the environment [2-4].

The application of quadrotor aircraft in agriculture has its advantages. The plant protection quadrotor aircraft operated by controllers has been recently applied to visually observe flight status. However, due to the failure of the mission operation, the flight status cannot be accurately monitored, and the safety of the flight operation and the task of monitoring environmental data cannot be guaranteed [5].

Scholars have conducted numerous studies on the impact of quadrotor aircraft on data acquisition, data exchange, and data monitoring in agricultural environment. However, problems on monitoring and trajectory optimization continue to exist. These issues reduce the monitoring efficiency of large-scale farmlands and affect the stability and accuracy of aircraft monitoring of agricultural environments.

On the basis of the preceding analysis, a design method for agricultural environmental monitoring based on the quadrotor aircraft is proposed by studying the principle of image recognition and trajectory optimization. In agricultural environmental monitoring, a quadrotor aircraft can realize independent flight according to positioning, navigation, trajectory optimization, and pattern recognition to collect high-definition images and videos of plants and analyze their growth status in real time.

2. State of the art

The use of quadrotor aircraft in farmlands has become increasingly relevant. However, the safety of its flight operation cannot be guaranteed [6]. A quadrotor aircraft has

*E-mail address: liby@dlpu.edu.cn
ISSN: 1791-2377
doi:10.25103/jestr.123.25

excellent performance and unique flight technology, but it also involves many problems, such as unstable acquisition of large-scale agricultural data, low data transmission efficiency, and low pattern recognition rate, which have been extensively studied by scholars. Chinese and international scientists have carried out relevant studies and considered several methods to solve the above problems.

In 1994, scientists from the Silsoe Institute in England implemented pattern recognition, measured and judged automatically the size and three-dimensional spatial coordinates of mushrooms through image processing, and selectively identified those mushrooms [7-8]. However, the research ignored the mushroom field with ample space, which could have offered reference value for pattern recognition.

In 1996, Kondo from the Okayama University developed a crop robot based on image processing through image recognition. The robot used a camera to collect images. The mature crops were identified, and the fruits and vegetables were monitored, after image processing. Problems on the accuracy of camera recognition have not been specifically solved, but the camera recognition algorithm has reference value [9-10].

In 2000, scholars in Israel developed a melon-picking robot by using black and white image processing methods to identify and locate melons in space. The robot can increase the probability of recognition success according to a particular geometric feature, such as the shape of melon as a circle or an ellipse. Their experiments showed that the picking robot can independently complete melon recognition [11].

In 2004, Zhang et al. from the China Agricultural University proposed an image segmentation algorithm for fruit object extraction by using a color space reference table. Through comparative experiments, the algorithm was applied to the image of a strawberry and a tomato under HSV and YCbCr color models, respectively, and they achieved ideal results [12-13].

In 2009, Song et al. from the Weifang University focused on of the spatial distribution information of eggplant growth and adopted the fixed threshold method based on the histogram to realize a small segmentation area of a gray image. They completed the judgment of the eggplant's contour, centroid, and other parameters. Their experiments showed that the method can achieve high recognition rates for eggplants, but their method is limited by the length of time needed to complete high-standard recognition [14-15].

In 2010, Si et al. from the Hebei Agricultural University recognized the apple images taken under different illumination conditions and obtained the outline image of the apple by using the normalized red–green difference algorithm. Their experimental results showed that the accuracy of the recognition algorithm can exceed 90%. At the same time, the random circle method was used to accurately extract the center and radius parameters of the fruits [16-17].

In an attempt to shorten the time of image recognition and improve the recognition rate of fruits, Lv et al. from the Changzhou University in 2014 realized the fast-tracking of target fruits by using the dynamic threshold segmentation method, developed the de-mean normalized product method, and carried out comparative experiments on fruit recognition. Their experimental results showed that the process can dramatically improve recognition rate [18-19].

In 2018, Xia et al. designed and implemented a quadrotor aircraft that can track, pick up, and transport to the target point independently. The analysis of its flight control principle indicates that the real-time altitude of the aircraft can be obtained by using an ultrasonic sensor, and the position of the aircraft can be judged by using computer image processing technology. The autonomous tracking flight and object recognition of the quadrotor aircraft are both realized and controlled by the proportion integral derivative (PID) controller, which can drive the manipulator to grasp and throw a target object [20].

In 2019, Qi et al. proposed a quadrotor aircraft based on a platform with STM32F407 microcontroller as the core. The hardware includes a nine-axis gyroscope sensor (MPU9150) for flight attitude information acquisition, an ultrasonic module (US100) for aircraft altitude and flight path image acquisition, and a camera module (OV7670) with a cloud platform that can be used for four-axis flight altitude and flight path elevation. The parameters were aimed to be corrected. Additionally, STM32F407 is added for image processing to improve real-time image acquisition and processing speed. Four-axis smooth flight and autonomous tracking can be achieved through attitude calculation, PID control algorithm, and real-time image processing [21].

On the basis of analysis of the above problems, a quadrotor aircraft with independent flight according to positioning, navigation, pattern recognition, and real-time transmission is proposed in this study. The quadrotor aircraft can monitor the agricultural environment and collect high-definition images of farmlands in real time and send back video information. Thus, the growth status of crops can be analyzed effectively, and the monitoring efficiency of the agricultural environment and the accuracy of crop image recognition can be improved.

The remainder of this study is organized as follows. Section 3 describes the quadrotor aircraft principle; establishes the control model of the quadrotor aircraft; presents the control algorithms of attitude calculation, pattern recognition, and processing; and discusses the designs of the software and hardware of the quadrotor aircraft. Section 4 presents the experimental measurement and the result of analysis. The last section summarizes the conclusions.

3. Methodology

3.1 Working principle of flight control algorithm

Flight stability is an important index in a quadrotor aircraft system, and the data acquired on aircraft attitude is the prerequisite of a stable flight. In large-scale agricultural environments, although a quadrotor can be used to investigate factors such as signal and weather interferences, an accurate measurement of flight attitude is impossible with a single attitude sensor, and the stability of the flight control system cannot be guaranteed. Therefore, the Kalman filtering algorithm is used to filter the data collected by the sensors [22-23]. Real-time flight attitude can be obtained by combining angular velocity data and acceleration data collected by MPU6050, and these data can be used to effectively reduce the impact of environmental noise on the aircraft system [24]. The flight control system process is shown in Figure 1.

In Figure 3.1, PMW-M# (#=1, 2, 3, 4) represents the output of four PWM signals in brushless electrical adjustment. The current motor throttle is calculated by the PID control algorithm and converted to a PWM signal to enable the electronic governor to control the motor rotation.

The diagram of the aircraft's software system is shown in Figure 2.

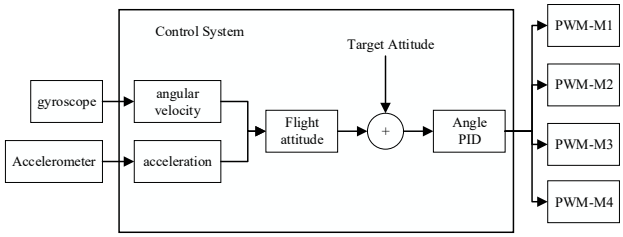

Fig. 1. Flight Control System Process

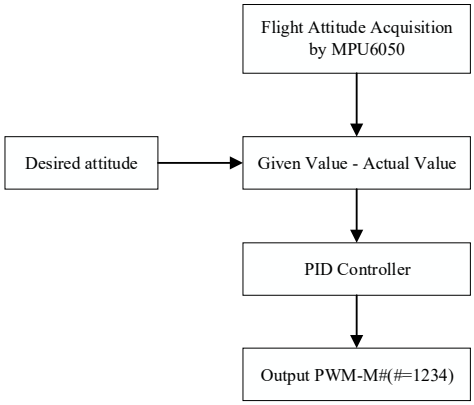

Fig. 2. The Diagram of the Aircraft's Software System

3.1.1 Kalman filter algorithm

The discretized differential equation of the attitude angle model of a quadrotor aircraft can be obtained, as shown in Equations 1 and 2.

$$x(k) = Ax(k-1) + BU(k-1) + W(k-1) \tag{1}$$

$$y(k) = Cx(k) + V(k) \tag{2}$$

where $x(k)$ is the system state at k-time; $U(k-1)$ is the control quantity of the system at k-time; A and B are parameters of the system; C is the parameter of the measuring system; and $W(k-1)$ and V(k) represent the control noise or process noise and the measurement noise, respectively.

The main equations of the Kalman filter are as follows.

State prediction:

$$\hat{x}(k|k-1) = Ax(k-1|k-1) + Bu(k-1) \tag{3}$$

State estimation:

$$p(k|k-1) = Ap(k-1|k-1)AT + Q \tag{4}$$

Filtering gain:

$$K(k) = P(k|k-1)CT / [CP(k|k-1)CT + R] \tag{5}$$

State optimization estimates:

$$\hat{X}(k|k) = x(k|k-1) + K(k)[Y(k) - Cx(k|k-1)] \tag{6}$$

Mean square error:

$$P(k|k) = [I - K(k)C]P(k|k-1) \tag{7}$$

The linear attitude model that consists of gyroscopes is obtained by the following state equation:

$$x(k) = \begin{bmatrix} 1 & -d \\ 0 & 1 \end{bmatrix} x(k-1) + \begin{bmatrix} di \\ 0 \end{bmatrix} u(k-1) + \begin{bmatrix} 0 \\ 1 \end{bmatrix} w(k-1) \tag{8}$$

$$\mathrm{z(k)} = [1 \quad 0]x(k) + vk \tag{9}$$

where $x(k) = \begin{bmatrix} \theta \\ b\theta \end{bmatrix}$, θ is the predicted angle, $b\theta$ is the error of angular velocity, dt is the sampling period, $U(k-1)$ is an angular velocity value of attitude change, $W(k-1)$ is the process noise, and $V(k)$ is the measurement noise. The gyroscope has excellent dynamic performance, can provide instantaneous progressive angle change, and is unaffected by acceleration change. By considering accumulated drift error, the use of a gyroscope only is unsuitable for long-time work.

$$\boldsymbol{x}_K = \begin{bmatrix} 1 & -di \\ 0 & 1 \end{bmatrix} \boldsymbol{x}_{k-1} + \begin{bmatrix} 0 \\ 1 \end{bmatrix} \boldsymbol{w}_{k-1} \tag{10}$$

$$\boldsymbol{z}_k = [1 \quad 0]\boldsymbol{x}_k + \boldsymbol{v}_k \tag{11}$$

The accelerometer has high measurement accuracy at rest, but it cannot accurately measure the change of angles during motion because of the influence of environmental factors. As a method for merging the advantages of gyroscope and accelerometer performance, the Kalman filtering algorithm is used to fuse and filter the signals, and the calculated data closest to the real value are used to improve the accuracy of the input data of the system [25].

3.1.2 PID control algorithm

The control system of the quadrotor aircraft adopts the PID control algorithm. The control module of the aircraft processes the collected data, calculates the current flight attitude, and subtracts the target flight attitude. The difference value is inputted to the PID controller for calculation, while the output PWM value is transmitted to the electronic governor to control the smooth flight of the quadrotor aircraft. An incremental PID algorithm is used for the attitude control of the aircraft control system [26]. Equation 12 is obtained by discretizing the incremental PID controller.

$$\mathrm{u}(k) = K_p e(k) + K_i \sum_{j=0}^{k} e(j) + K_d [e(k) - e(k-1)] \tag{12}$$

Incremental PID algorithm:

$$\begin{aligned} \Delta u(k) &= u(k) - u(k-1) \\ &= k_1 e(k) - k_2 e(k-1) + k_3 e(k-2) \end{aligned} \tag{13}$$

Here, T is the sampling period, T_d is a differential time constant, and T_i is an integral time constant. K_p, K_i, K_d

represent proportion, integral, and differential coefficient, respectively. $K_i = \frac{K_p T}{T_i}$ and $K_d = \frac{K_p}{T}$. K_1, K_2, K_3 are the correlation coefficient, $K_1 = K_p + K_i + K_d = K_p(1 + \frac{T}{T_i} + \frac{T_d}{T})$, $K_2 = K_p(1 + 2\frac{T_d}{T})$, and $K_3 = K_d$.

3.1.3 PID controller based on kalman filter

Figure 3 shows the structure of the PID control based on the Kalman filter processing. Matrices A, B, and C are determined by the debugging of the aircraft system. K is the amplification gain of the Kalman filter, y is the measurement signal disturbed by noise, and u is the output signal of the PID controller.

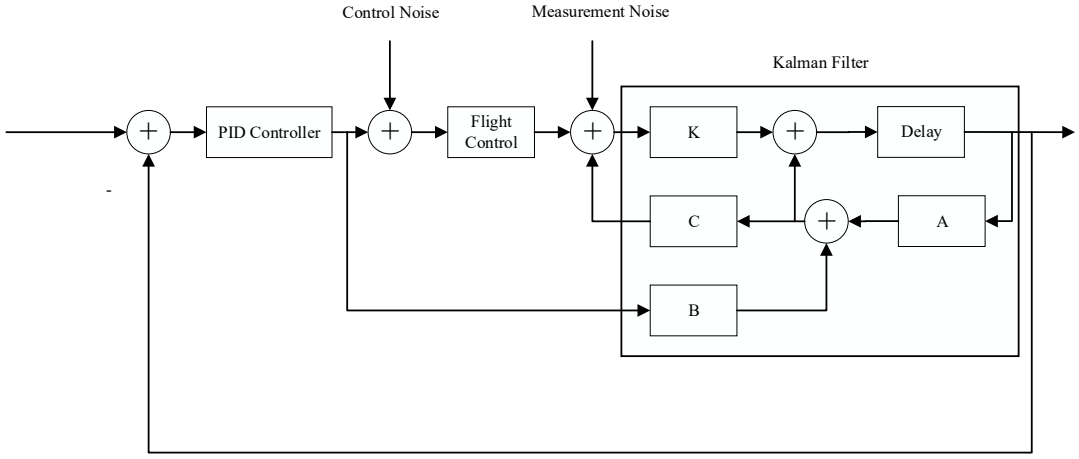

Fig. 3. The Structure of PID Control

Data units need to be unified by integrating the acceleration and angle values for attitude calculation to simplify the calculation process. First, the data collected by the accelerometer need to be converted into angle values. Considering the sampling time needed for computation, the angle value received by the gyroscope needs to be converted into angular velocity value. The Kalman filter calculates its amplification gain K according to the discretized state space equation of the system, variances P and Q of the disturbance noise, and the control signal u [27]. The amplification gain of the filter and the signal with interference noise are substituted into Equation 6 to obtain the Kalman filter signal, which is the value that the system predicts as the one closest to the real value. Equation 2 is used to calculate the filtered signal value. Subsequently, after subtracting the input signal of the aircraft system (the stable target attitude of the quadrotor aircraft), the difference value is transmitted to the PID controller. The control signal to be outputted by the aircraft system can then be obtained. The above calculation process is repeated until the target attitude of the aircraft in the system can be controlled [27].

3.2 Hardware design of quadrotor aircraft

The quadrotor aircraft control system uses STM32F03RET6 as the main controller [28-29]. The hardware of the control system consists of the minimum system of microcontroller, a power supply module, a flight attitude calculation module, a brushless electronic governor module, a brushless motor, a camera, a wireless communication module, and an image transmission module. The image transmission module provides large-scale agricultural image and video information about crop growth to the aircraft. The wireless communication module represents the hardware equipment for communication between the quadrotor aircraft and the ground station. The overall structure of the quadrotor aircraft system is shown in Figure 4.

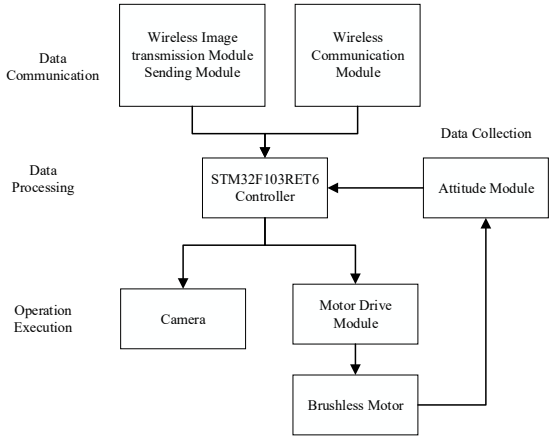

Fig. 4. Overall Structure Block Diagram of the Aircraft System

3.2.1 Power supply module

Different modules in the system have varying working voltages. Thus, the working voltage of each module needs to be designed to ensure regular operation. The working voltage of each module is shown in Table 1.

Table 1. Working voltage of each module

Working Module	Working Voltage of Each Module (V)
Controller	3.3 V
MPU6050	5 V
Wireless Image Transmission Module	5 V
Display OLED Module	3.3 V
Wireless Communication Module	3.3 V
Motor Drive Module	12 V

On the basis of the voltage requirement in Table 3.1, the DC–DC converter of the system operates in two-stage combination mode. The front stage uses an LM2596s-5 V chip to convert 12 V to 5 V, whereas the backstage uses an AMS1117-3.3V chip to reduce 5 V to 3.3 V.

3.2.2 DC (12 V to 5 V Circuit)

The DC with 5 V is generated by lowering the voltage of the LM2596S-5V chip, which is a switching voltage regulator chip. 12 V of input voltage can output a fixed voltage of 5 V. Up to 3 A of output current enables the circuit to drive more load. The DC, from a 12 V circuit to one that is 5 V, is shown in Figure 5.

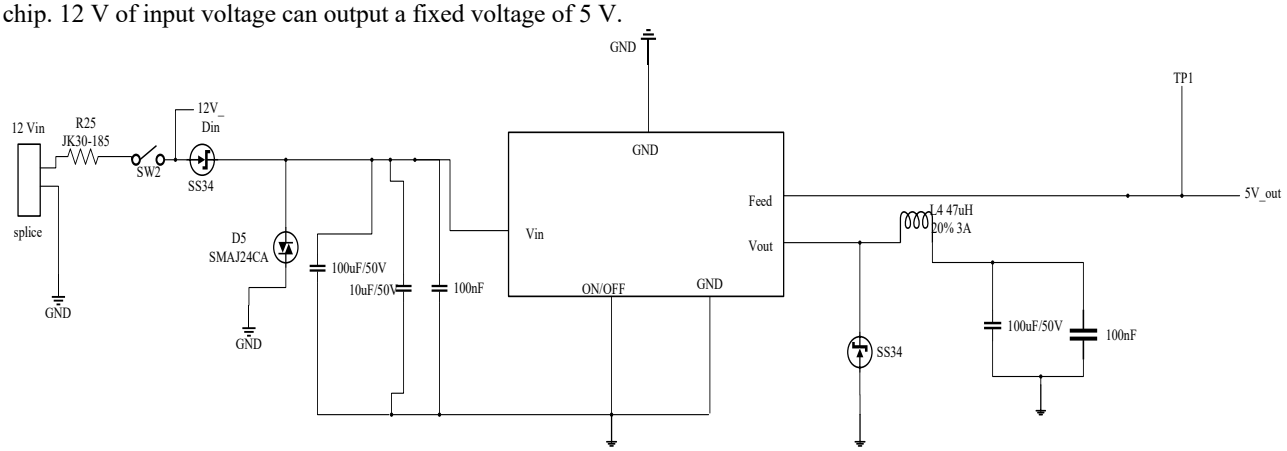

Fig. 5. DC (12 V to 5 V Circuit)

3.2.3 DC (5 V to 3.3 V Circuit)

The DC with 3.3 V is generated by the AMS1117-3.3 V chip, which is a forward low-voltage drop regulator. The chip integrates overheat protection and current limiting protection and can conveniently provide power to the system. AMS1117 is divided into fixed and adjustable versions. AMS1117-3.3 V is selected for this system to provide power for microcontrollers and to ensure the regular operation of the system. The DC, from a 5 V circuit to one that is 3.3 V, is shown in Figure 6.

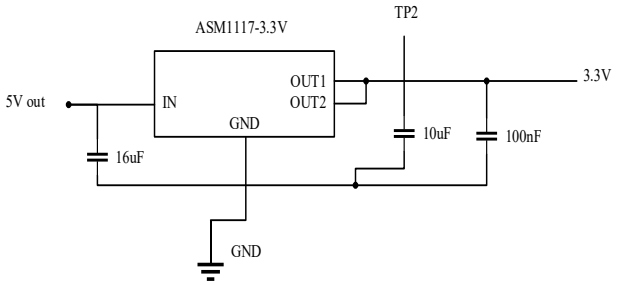

Fig. 6. DC (5 V to 3.3 V Circuit)

3.2.4 Flight attitude sensing module

The MPU6050 attitude acquisition module is the core of the hardware in the aircraft control system in this study. Data are transmitted through the STM32F103 serial UART, and MPU6050 is used as the output voltage signal for analogue-to-digital (AD) conversion to accurately output the attitude of the current system in real flight. Through attitude calculation, the angle, angular velocity, and acceleration of three axes (X, Y, and Z) can be obtained. Furthermore, combined with the dynamic Kalman filter algorithm, the attitude control accuracy can be improved by 0.01°, indicating a measurement accuracy that is much more stable.

3.2.5 Motor drive module

The quadrotor aircraft system uses four brushless motors, and the main control chip coordinates four brushless motors according to the flight attitude information collected by the MPU6050 gyroscope module. The output PWM control quantity is calculated by combining the navigation command and the control algorithm for the operation control of the four brushless motors to achieve stable flight. By controlling the duty cycle of the PWM output, speed of flight can be achieved by controlling the actual equivalent voltage added at both ends. The higher the duty cycle of the PWM is, the higher the equivalent voltage will be; the lower the duty cycle of the PWM is, the lower the equivalent voltage will be. The connection mode of the electric regulation is shown in Figure 7.

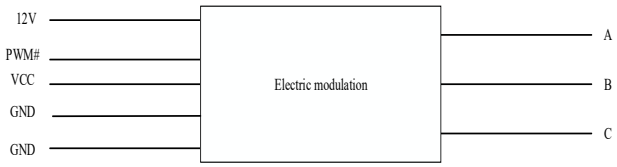

Fig. 7. The Connection Mode of Electric Regulation

3.2.6 Wireless communication module

The nRF24L01 wireless module operates in the ISM band of 2.4-2.5 GHz and has the function of automatic re-transmittance and automatic response. The quadrotor aircraft transmits the real-time image and video information of crops to the ground station through the wireless communication module.

3.3 Image processing

3.3.1 Image restoration

The camera carried by the quadrotor aircraft can capture crop image information at high altitudes. Given the changes in flight altitude and flight angle, the image captured by the camera from top to bottom has serious trapezoidal deformation in which the near image is much larger and the far image is much smaller. Images tend to differ from the object and appear to have specific features, such as combined trapezoidal and barrel distortions [31-32]. The captured image needs to be restored to the real picture to acquire real image information. The image processing system uses the inverse perspective transformation method to convert the plane image pixels (u, v) captured by the camera into (x, y) and restore the image in the three-dimensional coordinate system [33-34]. The principle diagram of the inverse perspective transformation is shown in Figure 8.

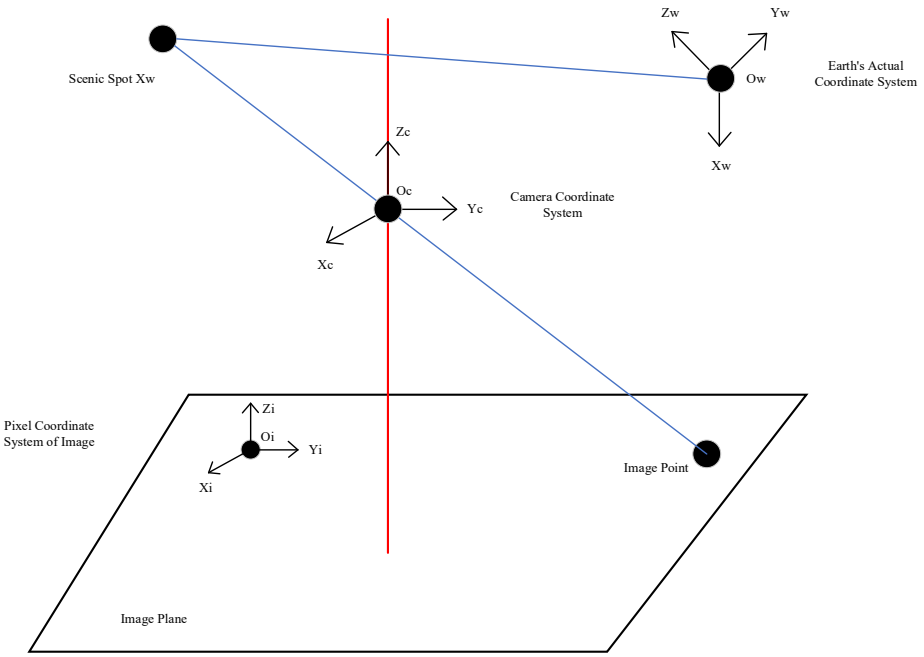

Fig. 8. Principle Diagram of Inverse Perspective Transformation

$U = MW$ can be obtained from the plane image pixel coordinate system $U(u,v,l)$ and the three-dimensional coordinate system $W(x,y,z,l)$. Then, the relational matrix M can be deduced. Equation 14 can be obtained by expanding the equation $U = MW$.

$$\alpha \begin{bmatrix} u \\ v \\ 1 \end{bmatrix} = M \begin{bmatrix} x \\ y \\ z \\ 1 \end{bmatrix} \tag{14}$$

Photography is the process of transforming a three-dimensional scene into a two-dimensional plane image. In the process of transformation, because of the different shooting angles, the corresponding relationship changes when the three-dimensional space is projected onto the two-dimensional plane. The process of inverse perspective transformation is opposite to that of photography. This kind of inverse change is highly complicated because it requires the transformation of a plane coordinate system and the three-dimensional coordinate system. The three-dimensional scene in the image processing system is reduced to a fixed two-dimensional plane [35] to simplify the process of inverse transformation.

In the process of shooting, Z coordinates are lost in three-dimensional coordinates (x, y, z). A basic assumption is that the ground covering of the crops is flat in the process of dimension reduction during inverse transformation.

If the ground is flat, then $Z = 0$. Equation 14 can be transformed into Equation 15.

$$\alpha \begin{bmatrix} u \\ v \\ 1 \end{bmatrix} = M \begin{bmatrix} \mathrm{x} \\ y \\ 1 \end{bmatrix} \tag{15}$$

Equation 16 can be deduced by further expanding Equation 15.

$$\begin{aligned} \alpha x &= n_{11}u + n_{12}\mathrm{v} + n_{13} \\ \alpha y &= n_{21}u + n_{22}\mathrm{v} + n_{23} \\ \alpha &= n_{31}u + n_{32}v + n_{33} \end{aligned} \tag{16}$$

Variable a is eliminated, and Equation 16 is written in matrix form as follows:

$$\begin{bmatrix} u & v & 1 & 0 & 0 & 0 & -ux & -vx \\ 0 & 0 & 0 & u & v & 1 & -uy & -vy \end{bmatrix} \vec{N} = \begin{bmatrix} x \\ y \end{bmatrix} \tag{17}$$

Where

$$\vec{N} = \frac{1}{n_{33}} \begin{bmatrix} n_{11} & n_{12} & n_{13} & n_{21} & n_{22} & n_{23} & n_{31} & n_{32} \end{bmatrix}^T \tag{18}$$

The aim is to calculate matrix N, and an effective approach is to calculate the corresponding coordinates of the four points. Equation 19 can then be obtained.

$$N' = \begin{bmatrix} n'_{11} & n'_{12} & n'_{13} & n'_{21} & n'_{22} & n'_{23} & n'_{31} & n'_{32} \end{bmatrix} \tag{19}$$

Equation 20 can be deduced from Equations 17 to 19.

$$\begin{aligned} x &= \frac{n'_{11}u + n'_{12}v + n'_{13}}{n'_{31}u + n'_{32}v + 1} \\ y &= \frac{n'_{21}u + n'_{22}v + n'_{23}}{n'_{31}u + n'_{32}v + 1} \end{aligned} \tag{20}$$

Therefore, the image coordinates (u, v) can be substituted into Equation 20 to obtain the actual three-dimensional coordinates (x, y), which is based on the premise of $Z = 0$.

3.3.2 Pattern recognition

The pattern recognition in this study uses the OpenCV camera module. The OpenCV–IDE interface is shown in Figure 9. This system needs to identify two colors of crop signs (red and green). RGB and LBA are commonly used in color analysis. The RGB color mode is a kind of color

standard in the industry. This mode can obtain different colors by changing the three-color channels of red (R), green (G), blue (B) and overlapping them. The L component of RGB matches brightness. Therefore, accurate color balance can be ensured by modifying the color order of elements a and b, or brightness contrast can be adjusted by using component L.

OpenCV mainly recognizes the LAB value of a color. Thus, the system defines the LAB value of two colors through the function of software color value selection. As shown in Figure 10, the lab value range is selected by dragging the maximum and minimum values of the corresponding lab values [36-37].

```
thr_blu = (15, 45, -10, 10, -10,10)
blobs = img.find_blobs([thr_blu)
```

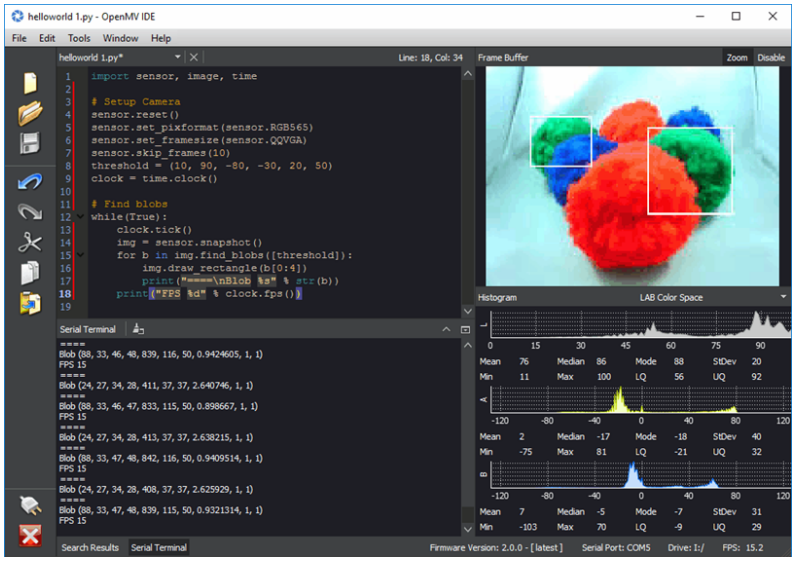

Fig. 9. OpenCV–IDE Interface

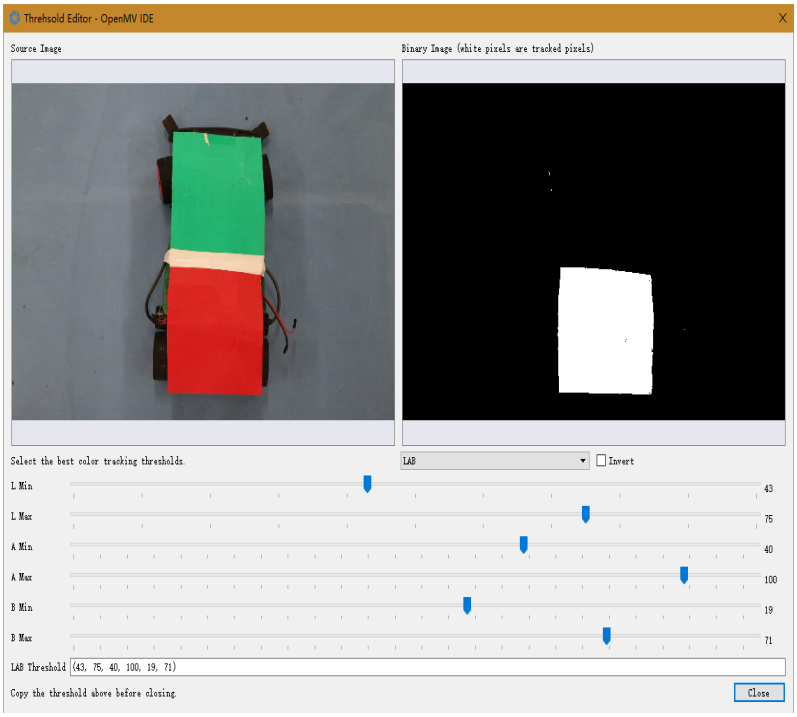

Fig. 10. Selection of Color Value of Symbols

The identified color needs to calculate the coordinates of the center point of the color block and send it to the main controller through the serial port. The resolution of the image is 320*240, and the abscissa is higher than 254. Thus, in the design of the system, the abscissa is divided into high eight bits and low eight bits to be sent separately.

```
# Get high eight digits
def get_high8(num):
    g_num=0
    g_num=num>>8
    return g_num
# Get low eight digits
def get_low8(num):
    g_num=0
    g_num=num&0xff
    return g_num
```

3.4 Software design of trajectory planning and data exchange

3.4.1 Program frame design

The program frame design of the flight control system is shown in Figure 11. The whole loop program is divided into three parts: received data, data processing, and data transmission. Received data are used to receive the coordinate data of symbols collected from the pattern recognition system. Data processing outputs the coordinate data to the flight control system through PID algorithm operation and then controls the aircraft to the scheduled position. Data transmission includes the parameters and states, such as flight direction, flight speed, flight time, and battery power, of the aircraft [38].

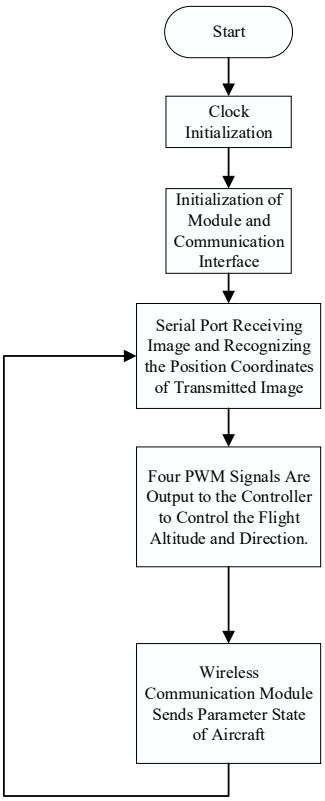

Fig. 11. Diagram of the Program Frame Design

3.4.2 Flight trajectory optimization programming

OpenCV can recognize a specified color and decorate the ground symbol into the specified color. The aim is to track the dynamic position change of the symbol. The OpenCV is mounted under the platform. Thus, the OpenCV's camera is always perpendicular to the ground regardless of the aircraft's rotation, and this configuration ensures that the measured data are accurate. When OpenCV appears in the range of detection, the coordinates of measurement must be outside the center point. The purpose of the actual measurement is to generate target point coordinates that are infinitely close to the center point coordinates. The resolution of the OpenCV camera is 320*240, and the set coordinates of the center point (or the expected coordinates) is (160,120). The camera is not fully installed in flight during real testing. Hence, the actual use of the central coordinates will be deviated because of the definite center of the device [36].

When the coordinates of the symbols are obtained, two approaches can be applied to make the aircraft move to the desired location. Two methods can be used to control the aircraft. The first method is to control the parameters in the yaw axis to change the heading, in which the nose of the quadrotor aircraft is in the direction of the symbol, and the pitch axis is controlled to achieve the purpose of controlling the aircraft for forward and back flight. The second method is to ignore the heading angle and instead control only the left and right flight of the aircraft, which can match the measured X-axis and Y-axis coordinates. The X and Y axes need separate PID operations and outputs for the pitch and roll axes, respectively [39-40].

The closed-loop control principle with PID algorithm for each axis is shown in Figure 12. First, the difference between the coordinates of the symbols and the desired coordinates obtained by the pattern recognition system is calculated for the position deviation. The advantage of this method is to eliminate the steady-state error of the system, mainly because the integration operation is required to accumulate the deviation for each time; however, the disadvantage is to reduce the stability of the system, and the response is too slow. Due to the massive inertia and fast response of the aircraft control system, position-based PD is used for the control system. The basic operation equations are shown below:

$$P_{out} = K_p * e(t) + K_d * (e(t) - e(t-1)) \tag{21}$$

where K_p is the proportional coefficient and K_d is a differential coefficient. $e(t)$ is the system error and $e(t-1)$ is the last systematic error.

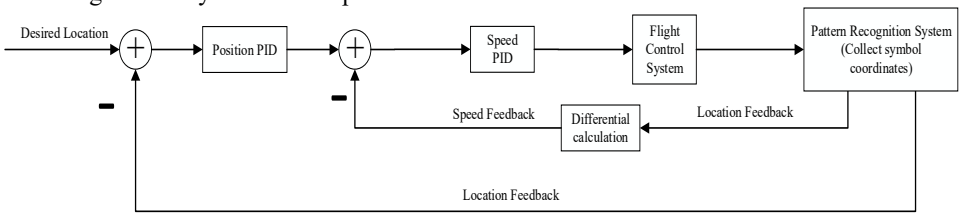

Fig. 12. Principle of double closed loop control

The position feedback is the coordinate of the measured symbol's position at this time, which differs from the expected coordinate, i.e., the systematic error is Err_x_1 (this error), whereas Err_x_2 is the second error. The equations are calculated by Equation 22:

$$\begin{aligned} exp\_x\_speed &= K_P\_POS\_x * Err\_x\_1 \\ &+ K_d\_POS\_x * \left(Err\_x\_2 - Err\_x\_1 \right) \end{aligned} \tag{22}$$

The output speed is regarded the expectation of the speed loop PID, and the difference between the two deviations is used as the speed feedback.

$Err\_x\_3 = Err\_x\_2 - Err\_x\_1$ is the speed feedback. The system's error of the speed loop PID can be obtained by Equation 23.

$$SpeedErr\_x\_1 = exp\_x\_speed - Err\_x\_3 \quad (23)$$

PD algorithm is performed again as follows:

$$Out\_pwm\_x = 937 - Kp\_SP\_x * SpeedErr\_x\_1 + Kd\_SP\_x * (SpeedErr\_x\_2 - SpeedErr\_x\_1) \quad (24)$$

where 937 is the PWM signal that derives the channel median.

Take the X-axis direction as an example, in which the Y-axis is the same. The procedure is as follows:

```
/****PID in X axis****/
float Kp_SP_x=5; // Speed Inner Loop PD
float Kd_SP_x=1;
float SpeedErr_x_1=0, SpeedErr_x_2=0;// Speed retention
float Err_x_1, Err_x_2,Err_x_3;
float exp_x_speed=0; //Outer
float Kp_POS_x=0.2; // Location Outer Loop PD
float Kd_POS_x=0;
float K
//Output----Speed
float out_pwm_x=0;    //Final Output
uint8_t set_var_x=150;
float Pid_x(float coor_x)
{
 Err_x_1 = set_var_x-coor_x ;
 Err_x_3=Err_x_2-Err_x_1;        //as the speed
exp_x_speed=KP_POS_x*Err_x_1+KD_POS_x*(Err_x_2-Err_x_1);
 Err_x_2=Err_x_1;
 SpeedErr_x_1=exp_x_speed-Err_x_3;
out_pwm_x=937-KP_SP_x*SpeedErr_x_1+KD_SP_x*(SpeedErr_x_2-SpeedErr_x_1);
SpeedErr_x_2=SpeedErr_x_1;
if(out_pwm_x>=1037) out_pwm_x=1037;
if(out_pwm_x<=837) out_pwm_x=837;
return out_pwm_x;
}
```

4 Result analysis and discussion

4.1 Distance and image sharpness analysis of quadrotor aircraft

A distance and image sharpness analysis of the quadrotor aircraft is performed in this study. After the system starts, the quadrotor aircraft controls the OpenCV camera to collect images of the area from the front end and then sends the collected images to the controller for image processing, including image binarization, image digital filtering, and fruit and vegetable feature point determination. The aircraft collects high-definition images of the agricultural environment and transmits the data of the farmland and related images back to the ground station by wireless communication. The altitude and position of the quadrotor aircraft can determine the stability and accuracy of video and image acquisition. The relationship between flight altitude and image recognition is shown in Table 2, while the relationship of flight altitude, air temperature, and humidity is depicted in Figure 13.

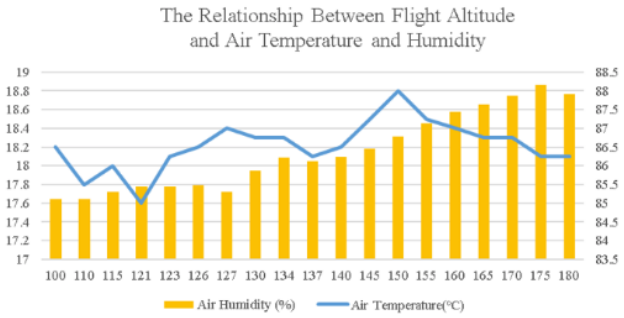

Fig. 13. Relationship of flight altitude, air temperature, and humidity

Table 2. The relationship between flight altitude and image recognition

Number	Flight Altitude of Quadrotor Aircraft (m)	Image Sharpness	Air Temperature (℃)	Air Humidity (%)
1	100	indistinctness	18.1	85.11
2	110	indistinctness	18.2	85.12
3	115	indistinctness	17.8	85.11
4	121	indistinctness	18.0	85.31
5	123	indistinctness	17.6	85.44
6	126	indistinctness	18.1	85.45
7	127	clear	18.2	85.49
8	130	clear	18.4	85.31
9	134	clear	18.3	85.87
10	137	clear	18.3	86.22
11	140	clear	18.1	86.12
12	145	clear	18.2	86.23
13	150	clear	18.5	86.45
14	155	clear	18.8	86.79
15	160	clear	18.5	87.14
16	165	clear	18.4	87.45
17	170	clear	18.3	87.64
18	175	clear	18.3	87.88
19	180	indistinctness	18.1	88.17
20	185	indistinctness	18.1	87.91

4.2 Image recognition of simulated agricultural Environment

With the image recognition and image transmission of the quadrotor aircraft, agriculture monitoring can be remotely performed on the basis of the rate of farmland recognition, air temperature, and humidity. Flight efficiency is approximately 82%, and the efficiency of aircraft image recognition is nearly 90%. The pattern recognition module is programmed and configured with Python language to realize the specified color recognition. The farmland environment is classified into the specified color by using OpenCV in the laboratory experiments, and the image with the specified

color is transmitted to the ground station. The color recognition tests at the same height are shown in Table 3, while the relationship between flight altitude and recognition success rate is shown Figure 14.

Fig. 14. Relationship between flight altitude and recognition success rate

Table 3. Statistical results of pattern recognition experiments

Number	Flight altitude of Quadrotor Aircraft (m)	Image Sharpness	Simulated Color	Image Recognition Color	Recognition success rate (%)
1	100	indistinctness	Red	Red	90.1
2	110	indistinctness	Green	Green	91.2
3	115	indistinctness	Red	Red	92.0
4	121	indistinctness	Green	Green	94.0
5	123	indistinctness	Red	Red	93.2
6	126	indistinctness	Green	Green	92.7
7	127	clear	Red	Red	97.8
8	130	clear	Green	Green	97.5
9	134	clear	Red	Red	97.6
10	137	clear	Green	Green	97.4
11	140	clear	Green	Green	98.8
12	145	clear	Red	Red	98.3
13	150	clear	Green	Green	98.1
14	155	clear	Red	Red	97.3
15	160	clear	Green	Green	97.7
16	165	clear	Red	Red	98.8
17	170	clear	Green	Green	98.9
18	175	clear	Red	Red	99.3
19	180	indistinctness	Green	Green	97.2
20	185	indistinctness	Red	Red	95.1

5 Conclusion

The problems of unpunctual collection of information of large-scale farmlands, long-range data return instability, and seasonal variation of the environment affecting crop growth are overcome in this study. In particular, a control system based on the quadrotor aircraft for agricultural environmental monitoring is proposed. The quadrotor aircraft, which involves pattern recognition and image video processing for farmland environment monitoring, collects high-definition images in real time and sends back videos. In this manner, the growth status of crops can be analyzed, and temperature, humidity, and other parameters of the atmospheric environment can be monitored regularly. An experimental study is subsequently carried out. The conclusions can be drawn as follows:

1)High-precision autonomous flight can be realized in the quadrotor aircraft system by positioning and recognizing the patterns of low-altitude ground symbols, thus ensuring the accuracy and reliability of the autonomous flight of the system.

2)The stability of the quadrotor aircraft is related to the regulation algorithm. The double closed-loop PID regulation algorithm can ensure the stability of the output force of the aircraft motor and reduce the fluctuation range of the aircraft.

3)The quadrotor aircraft can monitor the temperature and humidity of farmland and other environmental data. Wireless communication is used to transmit the images and videos of the farmland environment to the ground station.

4)The trajectory optimization algorithm can be applied to the quadrotor aircraft based on positioning and subsequently optimize the pattern recognition system, thus improving the accuracy of trajectory selection.

This study, which combines flight control experiment and quadrotor aircraft theory, proposes a design idea and implementation process for monitoring agricultural operations. The optimization of control algorithms, such as trajectory flight algorithm, image processing, pattern recognition, and environmental monitoring, offers a reference for the study and development of agricultural detection. Owing to the lack of a relatively large area (in hectares) of farmland environments in the real experiment, the data collected at present have certain randomness. In our future study, a much more accurate control is needed to cope with the complex situation and improve the recognition efficiency of aircraft.

References

1. Meng, Y. H., Zhou, G. Q., Wu, C. B., Wang, Z.G., Xu, C. D., "Discussion on the Application and Promotion of Agricultural Plant Protection UAV in China". *Journal of China Plant Protection Guide,* s1, 2014, pp. 33-39.
2. Ning, H. L., "Research on Binocular Vision-based Self-defined Gesture Recognition Method"., Doctoral Dissertation of Guangdong University of Technology, China, 2015, pp.1-61.
3. Wei, Z. X., "Design of wireless fire alarm system based on nRF24L01". *Journal of Electronic production*, 2014 (03), 2014, pp.53-55.
4. Li, Z. Y., "*Development of Computer Aided Design System for Fabric Pattern*". Doctoral Dissertation of Zhejiang University, China, 2010, pp.1-3.
5. Liu, G. C., "*Object recognition based on machine learning*". Doctoral Dissertation of Shanghai Jiaotong University, China, 2013, pp.1-165.
6. Van, H. E. J., Hemming, J., Van, T. J., "An autonomous robot for harvesting cucumbers in greenhouses". *Journal of Autonomous Robots*, 2002(13), 2012, pp.241-258.
7. Nobler., Reedjn., Miless., "Influence of mushroom strains and population density on the performance of a robotic harvester". *Journal of Agricultural Engineering Research*, 1997(68), 1997, pp. 215-222.
8. Reedjn., Miless., Butler., "Automatic mushroom harvester development". *Journal of Agricultural Engineering Research*, 78(1), 2001, pp. 15-23.
9. Kondo, N., Ting, K. C., "Robotics for plant production". *Journal of Artificial Intelligence Review*, 1998(12), 1998, pp. 227-243.
10. Kondon, N., Monta, M., Ogawa, Y., "Cutting providing system and vision algorithm for robotic chrysanhemum cutting sticking system". *Journal of Robotics and Mechatronics,* 1999, pp. 1-6.
11. Edany., Rogozind., Flasht., "Robotic melon harvesting". *Journal of Robotics and Automation*, 16(6), 2000, pp.831-835.
12. Zhang, T. Z, Lin, B. L., Gao, R., "Target extraction of fruit picking robot vision system". *Journal of China Agricultural University*, 2004(02), 2004, pp.68-72.
13. Zhang, K. L., Yang, L., Wang, G. B., Zhang, L. X., Zhang, T. Z., "Design and Test of Elevated Strawberry Picking Robot". *Journal of Agricultural Machinery*, 2012(09), 2012, pp. 165-172.
14. Song, J., Sun, X. Y., Zhang, T. Z., Zhang, B., Xu, L., "Design and experiment of open eggplant picking robot". *Journal of Agricultural Machinery*, 2009(01), 2009, pp. 143-147.
15. Song, J., "Vision recognition method of eggplant picking robot based on neural network". *Journal of Weifang University*, 2011(06), 2011, pp.90-93.

16 Si, Y. S., Qiao, J., Liu, G., Liu, Z. X., Gao, R., "Apple recognition and shape feature extraction based on machine vision". *Journal of Agricultural Machinery*, 2009(08), 2009, pp. 161-169, 173.

17. Si, Y. S., Qiao, J., Liu, G., Liu, Z. X., Gao, R., He, B., "Fruit recognition and location method of apple picking robot". *Journal of Agricultural Machinery*, 2010(09), 2010, pp. 148-153.
18. Lu, J. D., "*Research on visual measurement and obstacle avoidance control of apple picking robot*". Doctoral Dissertation of Jiangsu University, China, 2012, pp.1-169.
19. Lu, J. D., Zhao, D. A., Ji, W., "Fast positioning picking method of oscillating fruit by apple picking robot". *Journal of Agricultural Engineering*, 2012(13), 2012, pp.48-53.
20. Xia, H. J., Liu, H. N., Liu, T., Teng, F., "Research on the Autonomous Tracking and Material Retrieval Transportation System for Quad-Rotor Aircraft". *Journal of Jilin University (Information Science Edition)*, 37(1), 2019, pp. 1-10.
21. Qi, L., Wang, X., Li, X., Chen, W, L., Li, F. C., Peng, M. Y., Wang, C. H., Zhang, H. R., "Self-tracking Four-rotor design for PID control and image recognition". J*ournal of Microcontrollers and Embedded Systems*, 2018(9), 2018, pp.65-68.
22. Wei, Y. Z., Dong, X. L., "Design and analysis of an intelligent vibration isolation platform for reaction or momentum wheel assemblies". *Journal of Sound and Vibration*, 2012(13), 2012, pp.1-22.
23. Kamesh, D., Pandiy, R., Ashitava, G., "Modeling, design and analysis of low frequency platform for attenuating micro-vibration in spacecraft". *Journal of Sound and Vibration*, 329(17), 2010, pp. 3431-3450.
24. Xiao, B., Hu, Q. L., Michael. I, F., "Active fault-tolerant attitude control for flexible spacecraft with loss of actuator effectiveness". *International Journal of Adaptive Control and Signal Processing*, 2013(27), 2013, pp. 925-943.
25. C.J, Ran., Z.L, Deng., "Self-tuning distributed measurement fusion Kalman estimator for the multi-channel ARMA signal". *Journal of Signal Processing*, 2011(91), 2011, pp. 2028-2041.
26. Ye, S.Q., Zhan, L., "Attitude Control System of Four-Rotor Aircraft Based on PID". *Journal of Computer and Modernization*, 2015(05), 2015, pp. 117-120.
27. Wang, L., Zhang, Z., Wang, L., "An improved extended Kalman filter algorithm for attitude estimation of quadrotor". *Journal of Computer Applications*, 37(4), 2017, pp. 1122-1128.
28. Li, W.P., Tang, H.Y., "Research on attitude calculation of Four-rotor aircraft based on STM32". *Journal of Application of single-chip computer and embedded system*, 2016(06), 2016, pp.13-16.
29. Yan, P., Wang, L. D., Li, M. K., Hong, C. C., Jiang, D. F., "Design and implementation of a Four-rotor aircraft based on STM32". *Journal of Electronic Design Engineering*, 2016(2), 2016, pp. 187-189, 193.
30. Zhang, C. X., Li, T. Y., Wang, Y. L., "Design of Four-rotor flight control system based on MPU6050 and complementary filtering". *Journal of Sensing Technology*, 29(7), 2016, pp. 1011-1015.
31. Liu, G. G., Wu, Z. W., Liu, X., Li, H. P., "Pavement image restoration technology and experiment based on three-dimensional coordinate transformation". *Journal of CAAC University*, 2016(06), 2016, pp. 47-50.
32. Wu, Z.H., Zhang, P., Zhang, W., "Image acquisition and verification system based on OV7725 and serial port". *Journal of Information technology*, 2015(10), 2015, pp.90-92, 96.
33. Wang, C., Wang, H. A., Zhao, C. X., Ren, M. W., "Lane detection based on gradient enhancement and reverse perspective verification". *Journal of Harbin Engineering University*, 35(09), 2014, pp.1156-1163.
34. Wang, L.M., "Research on the Application of Open Source Computer Vision Library OpenCV". *Journal of public Communication of Science and Technology*, 2013(9), 2013, pp.224-225.
35. Sun, Y. L., Zhen, Z.Y., Wang, X. H., "Quad-Rotor Helicopter Target Tracking Based on Computer Vision". *Journal of Electronic Design Engineering*, 24(18), 2016, pp.159-161.
36. Qin, X.W., Wen, Z. F., Qiao, W.W., "Image Processing Based on OpenCV". *Journal of Electronic Test*, 2011(7), 2011, pp.39-41.
37. Teng, J., Wang, D. L., Wen, H.Y., "Visual C++ Digital Image Processing Method Based on OpenCV". *Journal of Modern Computer*, 2012(11), 2012, pp.70-72.
38. Kang, H., Zhao, K., Liu, S. L., "Design of Flight Attitude Recording System Based on MPU6050 Module". *Journal of Electronic Design Engineering*, 23(10), 2015, pp.188-190.
39. Yu, W. Q., "Design of Ultrasonic Range Finder Based on US-100". *Journal of Shandong Industrial Technology*, 2015(4), 2015, pp.147-194.
40. Mei, Z., Zhao, X.L., "The Intelligent Car Speed Regulation System Based on the Incremental PID". *Journal of Hubei University of Technology*, 30(2), 2015, pp.72-76.